

## THE MAGNETIC FIELD IN THE CONVECTION ZONE.

Alberto Bigazzi and Alexander A. Ruzmaikin

Jet Propulsion Laboratory, California Institute of Technology, CA USA

### ABSTRACT

One of the key questions in solar physics that remains to be answered concerns the strength and the distribution of the magnetic fields at the base of the convection zone. The flux tube dynamics requires that toroidal fields of strength as large as 100 kilogauss be present at the base of the convection zone. The kinetic-magnetic equipartition argument leads to smaller field strengths. For possible detection of these relatively small (compared to pressure effects) fields by helioseismic methods it is important to know the range of the field strengths and their distribution.

We estimate a range for the toroidal magnetic field strengths at the base of the convection zone using dynamo simulations in a spherical shell. These simulations involve the distribution of rotation provided by helioseismic inversions of the GONG and MDI data. Combining the simulations with the observed line-of-sight surface poloidal field we extract the spatial pattern and magnitude of the mean toroidal magnetic field at the base of the convection zone.

### 1. INTRODUCTION

The inner distribution of the solar magnetic field is poorly known. Despite the striking regularity of the solar activity, we still lack an understanding of its causes and the mechanisms by which it operates.

The layer that we are able to directly observe the magnetic fields on is the photosphere. From observations of sunspots we know that magnetic fields with intensities of the order of thousands of Gauss are produced somewhere below the photosphere and can live for months before decaying away. The topological and magnetic structure of sunspots (as expressed by Hale's and Joy's laws) suggest that they harbor intense, toroidal magnetic flux tubes. The poloidal component of the solar magnetic field is much weaker compared with the toroidal field.

The intensity and spatio-temporal distribution of magnetic fields inside the Sun represent a challenge for any theory explaining the origin of solar activity. On one hand, the highly localised sunspot field points toward

local dynamics. On the other, the much more diffuse poloidal field more naturally fits into a mean-field model. One needs to combine two approaches to explain the solar cycle: the flux tube dynamics and the mean field dynamo. Thin flux tube dynamics has been very successful in explaining features connected to sunspots, see e.g Choudhuri & Gilman 1987, Fan Fisher & De Luca 1993, Caligari, Moreno-Insertis, & Schüssler 1995. The periodic migration of sunspots toward the equator and the field reversal cannot be explained by this dynamics alone. The explanation of the reversals of the field and of the equator-ward migration of the activity were in fact one of the great achievements of the mean field dynamo theory originated by Parker, Steenbeck, Krause and Rädler (Parker 1955, Steenbeck, Krause and Rädler 1969). Yoshimura (1975a) proved that waves mainly propagate along the isosurfaces of angular velocity. With the present knowledge of solar differential rotation, this would imply that inside the bulk of the convection zone waves travel radially outwards, not giving rise to equator-ward migration. Migration may be restored in the shear layer at the base of the convection zone.

While it is possible to generate high magnetic fluxes by means of differential rotation, to store them for enough time to allow for their intensity to build up would not be feasible in the convection zone because such magnetic flux tubes would erupt in a timescale of months (Parker 1975, Moreno-Insertis 1986). Helioseismology tells us that around  $0.7 R_{\odot}$ , a sharp radial change in the solar rotation curve happens in a layer whose thickness can be as small as  $0.02 R_{\odot}$  (see Christensen-Dalsgaard et al. 1991, Basu & Antia 1997, Kosovichev 1996, Corbard et al. 1998, Charbonneau et al. 1999. ).

The same layer may allow for fields up to  $10^5$  Gauss to be stored, what would be needed for thin flux tube dynamics to work in the case of the Sun (Moreno-Insertis et al. 1992, Ferriz-Mas & Schüssler 1994)

Following Ivanova & Ruzmaikin (1977), Parker (1993) discussed a model of mean field dynamo that includes a sharp gradient of turbulent diffusivity and two distinct location for the sources of the magnetic field, that is differential rotation and helical turbulent motions. Stronger toroidal fields can in fact be produced in the region where diffusivity is smaller, just below the convection zone. Separating the shear layer and the source of the alpha-effect, moreover, would allow for alpha not be quenched

by the strong underlying magnetic field. A very thorough investigation of this kind of models has been carried out by Charbonneau and MacGregor, 1997. We will use in our Profile II a similar setup to one of those discussed in the aforementioned paper.

In the following, we are going to study how different profiles of the  $\alpha$ -effect may influence the spatial distribution of fields. We shall consider the profile of diffusivity and the rotation curve as given.

Mean field, kinematic dynamo cannot predict the absolute values of the generated magnetic fields, only their ratio. The measured mean radial field at the surface can then be used to infer the value of the toroidal magnetic field in the interior, once the ratio is known.

## 2. DYNAMO MODEL

We consider axisymmetric solutions of the mean field dynamo. We assume for the solar rotation a simple analytical fit to the profile reconstructed by helioseismic where the surface rotation curve

$$\Omega_s = \Omega_{\text{Eq}} (1 + a_1 \cos^2 \theta + a_2 \cos^4 \theta) \quad (1)$$

is made smoothly match the core rotation  $\Omega_c$  in a layer of thickness  $0.2R_\odot$  at  $0.692R_\odot$ . Equatorial rotation is  $\Omega_{\text{Eq}} = 2.865 \times 10^{-6} \text{s}^{-1}$  and the core rotation taken as the value of  $\Omega_s$  at  $30^\circ$  latitude.  $\theta$  here is colatitude.  $a_1 = -0.126$  and  $a_2 = -0.159$ . The radial profile of  $\partial\Omega/\partial r$  at the equator is shown in solid line in Figure 1. The sign of this gradient is opposite at higher and lower latitudes. Turbulent diffusivity  $\eta$  is constant throughout the Convection Zone and we have it drop a factor 10 to 50, in a layer of thickness  $0.2R_\odot$  at a location either coincident with that of the rotational shear layer or slightly above it, at  $0.713R_\odot$ . Both these values have been worked out in the context of Helioseismology, see Christensen-Dalsgaard et al. 1991, Basu & Antia 1997, Kosovichev 1996, Corbard et al. 1998, Charbonneau et al. 1999. In reality the drop in turbulent diffusivity is estimated to be of the order of  $10^6$ . In Figure 1 the diffusivity profile along the radial direction is represented by the solid dashed line, its gradient marking the bottom of the Convection zone. In solid line, the radial derivative of the rotation which defines the shear layer is plotted.

The mean field dynamo equation, written in terms of scalar potentials (Krause & Rädler, 1980) is solved numerically in a  $r - \theta$  meridional semi-disk. Second order finite differences in space and a third order Runge-Kutta scheme for time advance are used. In most of the runs a grid of  $60 \times 40$  is used. Ideal conductor boundary conditions are used at the interface with the core and radial field condition is implemented at the surface. Regularity condition are imposed on the axis.

No model for non-linear  $\alpha$ -quenching has been used. This is consistent with our assumption that the flow field is not influenced by the magnetic field.

### 2.1. The $\alpha$ -effect

Given the lack of constraints on the form of the  $\alpha$ -effect, we shall discuss how different alphas influence the spatial distribution of the the toroidal and poloidal fields. Figure 1 shows the distribution in radius of  $\alpha$ . In all models, a latitudinal dependence of  $\cos(\theta)$  is included. This is standard in dynamo theory and reflects the property of the alpha-effect of being antisymmetric with respect to the Equator. In case IV, an additional factor of  $\sin^2(\theta)$  is present. This has been discussed by Rüdiger & Brandenburg, 1995, and has the effect of shifting the magnetic field patterns closer to the equator, which better reproduces the observed patterns of sunspot migration.

Profile I, the diamonds in Figure 1, is maximum in the bulk of the Convection Zone, at  $0.82 R_\odot$  in our case. It is null at the surface. This form of the  $\alpha$ -effect takes into account the influence o the rotation on helical turbulence, see Zeldovic, V. Ruzmaikin, Sokoloff 1983. Profile II, squares, is sharply peaked at  $0.7 R_\odot$ , just above the shear layer, and represents an Interface Dynamo model. As already mentioned, this profile was used by Charbonneau and MacGregor (1997). Profile III is, instead, non vanishing only in the outer shell of the Convection Zone. This kind of “surface dynamo” has been discussed in conjunction with meridional circulation, see e.g. Choudhouri et al. 1995. Profile IV, triangles, has a constant value throughout the whole Convection Zone. It drops to zero close to the surface and at the base of Convection Zone. This profile has often be adopted in the literature. The last case considered, V,  $\alpha$  has two contributions: one coming from the bottom of the convection zone where it is negative and proportional to the gradient of  $\eta$ , combining the effects due to the the decrease in the intensity of the turbulence and the stratification. The other, coming from the convection zone, is taken to be the same as in I. Yoshimura (1975b) has used this form for the  $\alpha$ -effect.

| $\alpha(r)$ | $r_\alpha$ | $\alpha_0$ | $\gamma$ | $T$  | $r_{\text{max}}$ | $B_t/B_r$ |
|-------------|------------|------------|----------|------|------------------|-----------|
| I           | .75        | 4.1        | 8.2      | .026 | .71, .84         | 310       |
| II          | .7         | 27.5       | 19       | .047 | .67, .80         | 950       |
| III         | > .8       | 4.1        | 18       | .008 | .78, .92         | 36        |
| IV          | .7 ÷ .98   | 4.23       | 5        | .015 | .9               | 73        |
| V           | .75        | 5          | 180      | .020 | .71              | 360       |

Table 1. Location and intensity of the maximum toroidal magnetic field for different choices of the profile of the  $\alpha$ -effect. The location where the profile is peaked  $r_\alpha$  is given, along with the intensity  $\alpha_0$ .  $\gamma$  and  $T$  are the growth rate and the period of the solutions.  $B_r$  is the maximum value of the radial photospheric field averaged over time.  $B_t$  is the maximum value of the time average of the toroidal magnetic field intensity. When two values are given, the first one represents a secondary maximum close to the shear layer, see Figure 2.  $r_{\text{max}}$  is the location where the maximum is located, in units of  $R_\odot$ . Numbers are adimensional. Lengths have been scaled to  $R_\odot$  and time to  $R_\odot^2/\eta$ , where  $\eta$  is the value of turbulent diffusivity in the convection zone.

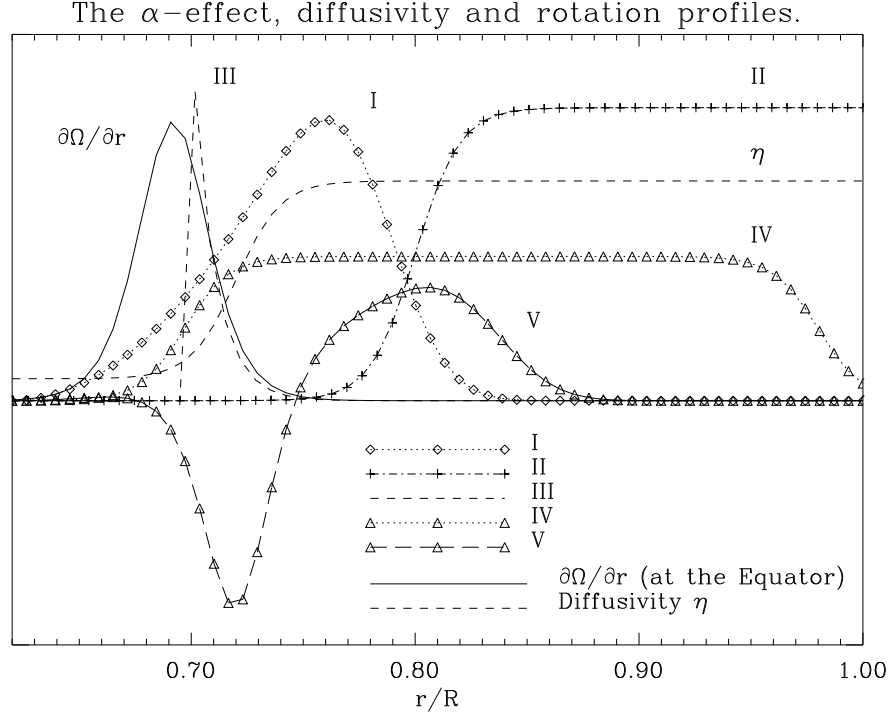


Figure 1. Radial distribution of the  $\alpha$ -effect for the cases I-V. Values are not to scale. See Table 1 for the actual values used in the present simulations. The solid lines, dashed and continuous, represent the radial profile of the turbulent magnetic diffusivity  $\eta$  and the radial gradient of the rotation rate  $\partial\Omega/\partial r$  at the equator, respectively. They define for our model the Convection Zone and the shear layer (the Tachocline).

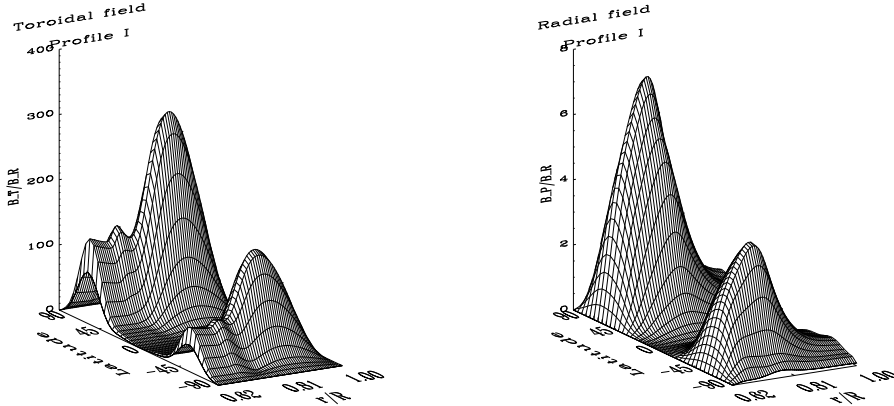


Figure 2. Surface plot of toroidal and radial field intensity integrated over time for Profile I. Values are scaled to the maximum of the radial surface field.

### 3. DISCUSSION OF THE RESULTS

Except for the case of Profile III, where  $\alpha$  is concentrated in the surface layer, all the case studied display a local maximum of the toroidal field in the shear layer. Except for case V, this is not an absolute maximum which is instead achieved in the convection zone, within  $0.8 \div 0.9 R_\odot$ , see Figure 2 and Figure 3.

The ratio of the maximum toroidal field to the surface radial field can vary from a few tens as in the case of the surface  $\alpha$ -effect, case III, to a thousand, as in the case of

the interface profile II. Both the profile I and V have ratios of the order of a few hundreds. No symmetry across the equator has been imposed on the solution which display a North-South asymmetry. Except for case of the surface  $\alpha$ , the symmetry of the solution is mainly dipolar. Considering a mean radial surface field of the order of a Gauss (Schlichenmaier and Stix 1995) the range of ratios that we found would lead to an estimate of the large-scale mean toroidal field of the order of  $10^3$  Gauss in the most favorable cases I,II,V. Both the surface (III) and top-hat (IV) profiles have smaller ratios of the toroidal to the surface fields.

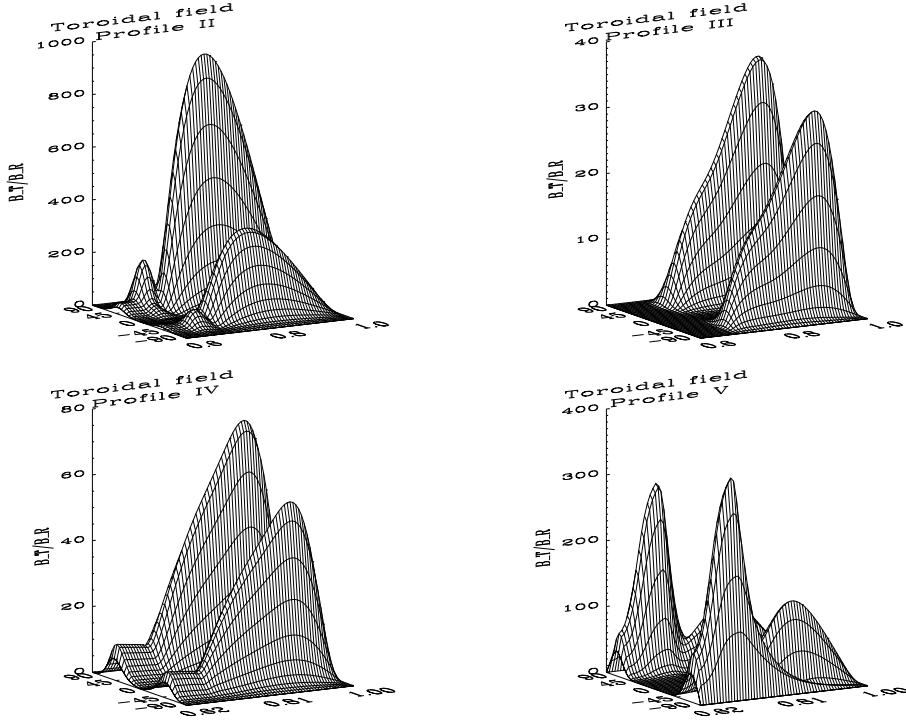


Figure 3. Toroidal fields for Profile II-V. Values are scaled to the maximum of the radial surface field.

If one assumes that solar activity is originated in the shear layer, then it is possible to draw a *butterfly diagram* with the temporal evolution of the toroidal field near the shear layer. All those models show butterfly diagrams with activity at higher latitude than observed. This is a known feature of many dynamo models.

We have shown that different assumptions about the  $\alpha$ -effect give rise to very different spatial distributions of the magnetic fields inside the Sun. This message could also be read in reverse: should we be able to probe the field deeply inside the Sun, we could have information about the nature of the regeneration mechanism expressed by the  $\alpha$ -effect.

#### ACKNOWLEDGMENTS

This work was performed while A. Bigazzi held a National Research Council Research Associateship Award at the Jet Propulsion Laboratory. This research was conducted in part at the Jet Propulsion Laboratory, California Institute of Technology, under contract with NASA.

#### REFERENCES

Fan, Y., Fisher, G. H., Deluca, E. E., 1993, ApJ 405, 390  
 Choudhuri, A.R., Gilman, P. A., 1987, ApJ 316, 788  
 Parker E.N., 1975, ApJ 198, 205  
 Moreno-Insertis F., 1986, A&A 166, 291  
 Moreno-Insertis, F., Schüssler M., Ferriz-Mas, A., 1992, A&A, 264 686

Ferriz-Mas A., Schüssler M., 1994, ApJ, 433, 852  
 Parker, E. N., 1955, ApJ. 122, 293  
 Steenbeck, M., Krause F., Rädler K.-H., 1966, Z. Naturforsch., 21a, 369  
 Parker, E.N., 1993 ApJ 408, 707  
 Ivanova, T.S., Ruzmaikin A., 1977, Sov. Astronom. 21, 479  
 Krause F., Rädler K.-H., 1980, Mean-field Magnetohydrodynamics and dynamo theory, Akademie Verlag, Berlin.  
 Rüdiger G., Brandenburg A., 1995, A&A, 296, 557  
 Yoshimura H., 1975a, ApJ 201, 740  
 Yoshimura H., 1975b, ApJs 294, 29, 467  
 Zeldovic Ya.B., Ruzmaikin A.A., Sokoloff D.D., 1983 Magnetic Fields in Astrophysics, Gordon and Breach.  
 Choudhuri, A.R. Schüssler, M., Dikpati M., 1995, A&A, 303, L29  
 Charbonneau P., MacGregor K.B., 1997, ApJ 486, 502  
 Caligari P., Moreno-Insertis F., Schüssler M., ApJ 441, 886  
 Christensen-Dalsgaard J. Gough D.O., Thompson M.J., 1991, ApJ 378, 413  
 Basu S., Antia H., 1997, MNRAS 287, 189  
 Kosovichev A.G., 1996, ApJ 469 L61  
 Corbard, T., Berthomieu, G., Provost, J., Morel, P., 1998, A&A, 330, 1149  
 Charbonneau, P., Christensen-Dalsgaard, J., Henning, R. et al., 1999, ApJ 527, 445  
 Schlichenmaier R., Stix M., 1995, A&A 302, 264